

Valence evaluation of LiMnO₂ and related battery materials by x-ray absorption spectroscopy

H. Wadati,^{1,*} D. G. Hawthorn,² T. Z. Regier,³ G. Chen,⁴
T. Hitosugi,⁵ T. Mizokawa,⁶ A. Tanaka,⁷ and G. A. Sawatzky¹

¹*Department of Physics and Astronomy, University of British Columbia, Vancouver, British Columbia V6T 1Z1, Canada*

²*Department of Physics and Astronomy, University of Waterloo, Waterloo, Ontario N2L 3G1, Canada*

³*Canadian Light Source, University of Saskatchewan, Saskatoon, Saskatchewan S7N 0X4, Canada*

⁴*Department of Materials Science, College of Materials Science and Engineering,
Jilin University, Changchun 130012, People's Republic of China*

⁵*WPI Advanced Institute for Materials Research (WPI-AIMR), Tohoku University, Sendai 980-8577, Japan*

⁶*Department of Complexity Science and Engineering,
University of Tokyo, Kashiwa, Chiba 277-8561, Japan*

⁷*Department of Quantum Matters, ADSM, Hiroshima University, Hiroshima 739-8530, Japan*

(Dated: April 28, 2021)

We present an x-ray absorption study of the oxidation states of transition-metal-ions of LiMnO₂ and its related materials, widely used as cathodes in Li-ion batteries. The comparison between the obtained spectrum and the configuration-interaction cluster-model calculations showed that the Mn³⁺ in LiMnO₂ is a mixture of the high-spin and low-spin states. We found that Li deficiencies occur in the case of Cr substitution, whereas there are no Li deficiencies in the case of Ni substitution. We conclude that the substitution of charge-transfer-type Ni or Cu is effective for LiMnO₂ battery materials.

Many current electrodes of rechargeable Li batteries have layered structures. Among them, a layered transition-metal oxide Li_xCoO₂, in which the concurrent insertion of Li in a crystal structure and the reduction of the Co ions is achieved [1], has become widely used as a cathode electrode in the batteries in most portable electronics. Since then, much effort has been made to enhance charge/discharge rates of the cathode material and/or to replace Li_xCoO₂ by less expensive Li_xMnO₂ or related materials. In addition, in the recent ab-initio computational modeling study, LiNi_{0.5}Mn_{0.5}O₂ is proposed as a next generation cathode material with high power and high capacity applications [2]. Although the valence states and local electronic configurations of the transition-metal ions are related to the charge/discharge rates, no systematic spectroscopic study has been performed to identify their local electronic configurations experimentally. Here, we report a systematic x-ray absorption spectroscopy (XAS) study of LiMnO₂, LiNi_{0.5}Mn_{0.5}O₂, and related compounds which are thought as future cathode materials. The present experiment and theoretical analysis reveal that LiMnO₂ has the Mn³⁺ site with the unexpected degeneracy between the low-spin (LS) and high-spin (HS) states and that LiNi_{0.5}Mn_{0.5}O₂ consists of HS Ni²⁺ and Mn⁴⁺. In the case of LiMnO₂, small perturbation such as Cr doping may stabilize the LS Mn³⁺ state. These results show the potential of LiMnO₂ and LiNi_{0.5}Mn_{0.5}O₂ for use as cathode materials and provide fundamental information that can be used for the development of new Li-ion batteries for high power applications.

LiCoO₂, LiMnO₂, and LiNi_{0.5}Mn_{0.5}O₂ have the layered structure as schematically shown in Fig. 1 (a). In

this structure, the O²⁻ ions provide a framework with face-centered cubic structure and Li⁺ and transition-metal ions occupy all the octahedral interstices, leading to alternate two-dimensional triangular lattice layers. Under the octahedral crystal field, the five-fold transition-metal 3d level is split into two-fold e_g and three-fold t_{2g} levels. In these layered cathode materials, the Li⁺ ions diffuse between the octahedral sites through the tetrahedral interstices. In LiCoO₂, the pathways of Li⁺ ions are in contact with the LS Co³⁺ in which the t_{2g} orbitals are fully occupied (t_{2g}^6). After the charging process, the LS Co³⁺ (t_{2g}^6) is partly changed into the LS Co⁴⁺ (t_{2g}^5), in which the structural change by the oxidation is minimal. The electronic configurations of these two Co ions are shown in Fig. 1 (b). If the Mn³⁺ ion in LiMnO₂ and the Mn⁴⁺ ion after the charging process take the electronic configurations of LS t_{2g}^4 and t_{2g}^3 , respectively, as recently indicated by ab-initio calculation [3], the structural change by the oxidation is also expected to be minimal. If the Mn³⁺ ion in LiMnO₂ takes the HS configuration with one e_g electron, the Mn octahedral site should be deformed by Jahn-Teller effect to lift the two-fold degeneracy of the e_g levels. In such case, local structural change during the charging process is substantial, leading to poor charge/discharge rate as well as poor charge/discharge cycle lifetime. The electronic configurations of these three Mn ions are shown in Fig. 1 (c). In LiNi_{0.5}Mn_{0.5}O₂, half of the Li⁺ activated sites are in contact with Ni²⁺ and higher Li diffusivity is expected. If the Ni²⁺ ion in LiNi_{0.5}Mn_{0.5}O₂ and the Ni⁴⁺ ion after the charging process take the HS configuration $t_{2g}^6 e_g^2$ and the LS configuration t_{2g}^6 , respectively, both of these ions are Jahn-Teller inactive.

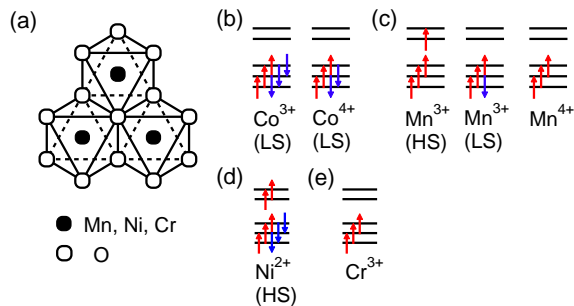


FIG. 1: (Color online) Crystal structure of cathode materials (a) and electronic configurations. (b) Co^{3+} (LS) and Co^{4+} (LS). (c) Mn^{3+} (HS), Mn^{3+} (LS) and Mn^{4+} . (d) Ni^{2+} (HS). (e) Cr^{3+} .

As discussed in the previous paragraph, the local electronic configuration of the transition-metal ions is highly important to determine the electrochemical properties of the cathode materials. In this report, we present a systematic XAS study of the cathode materials to extract fundamental information on their electronic configurations. We determined the valence of transition-metal ions by XAS and discussed what type of substitution is most suitable for LiMnO_2 batteries.

The powder samples of LiMnO_2 , $\text{LiMn}_{0.5}\text{Ni}_{0.5}\text{O}_2$, and $\text{LiMn}_{0.65}\text{Cr}_{0.35}\text{O}_2$ were synthesized by the procedure described in Refs. [3, 4]. The powder of LiMnO_2 and $\text{LiMn}_{0.5}\text{Ni}_{0.5}\text{O}_2$ have a monoclinic structure, while $\text{LiMn}_{0.65}\text{Cr}_{0.35}\text{O}_2$ has a rhombohedral (α - NaFeO_2 -type) one. XAS experiments were performed at 11ID-1 (SGM) of the Canadian Light Source. The spectra were measured in the total-electron-yield (TEY) mode. The obtained TEY spectra were similar to the partial-fluorescence-yield spectra. The resolution power ($E/\Delta E$) was set to 5000. All the spectra were measured at room temperature.

Figure 2 (a) shows the Mn $2p$ XAS spectra and their comparison with the reference data of Mn^{2+} (MnO), Mn^{3+} (LaMnO_3), and Mn^{4+} ($\text{EuCo}_{0.5}\text{Mn}_{0.5}\text{O}_3$ and SrMnO_3) from Ref. [5]. The spectra of $\text{LiMn}_{0.5}\text{Ni}_{0.5}\text{O}_2$ and $\text{LiMn}_{0.65}\text{Cr}_{0.35}\text{O}_2$ are very similar to those of the Mn^{4+} references, indicating that the valence of Mn is $4+$ in these materials. The spectrum of LiMnO_2 is different from the other three results and also from the Mn^{2+} and Mn^{4+} references. It is similar to the Mn^{3+} reference of LaMnO_3 , but the lineshapes are slightly different. We considered that this difference may come from the spin states, that is the difference between HS and LS states, and performed configuration-interaction (CI) cluster-model calculations [6]. Figure 2 (b) shows the comparison with the CI theory. The value of the crystal field splitting between e_g and t_{2g} states, $10Dq$, was changed from 1.0 eV to 2.0 eV. The positive value of

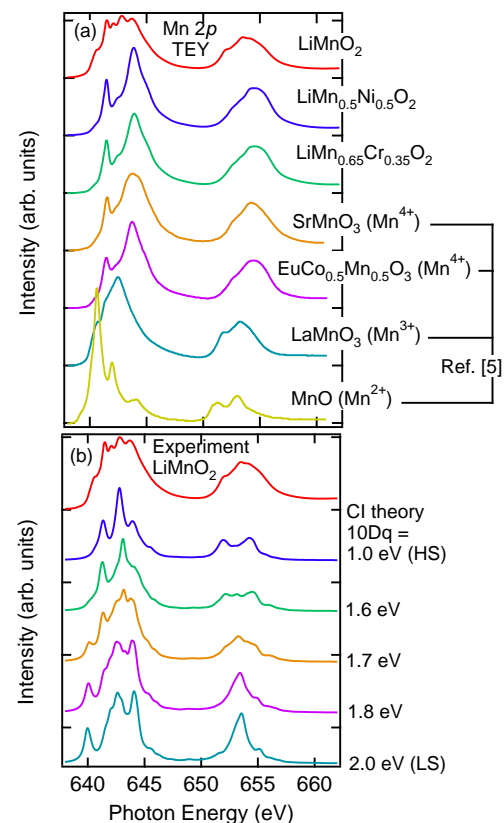


FIG. 2: (Color online) (a) Mn $2p$ XAS spectra and their comparison with the reference data of Mn^{2+} (MnO), Mn^{3+} (LaMnO_3), and Mn^{4+} ($\text{EuCo}_{0.5}\text{Mn}_{0.5}\text{O}_3$ and SrMnO_3) from Ref. [5]. (b) Comparison with the CI theory.

$10Dq$ means that e_g states have a higher energy than t_{2g} , which is the case in the MnO_6 octahedral coordination as shown in Fig. 1 (a) [7]. The increase of $10Dq$ from 1.0 eV to 2.0 eV corresponds to the transition from HS to LS states. (The electron configurations are shown in Fig. 1 (b)). The spectrum of LaMnO_3 in Fig. 2 (a) is in good agreement with the results of CI theory with $10Dq = 1.0$ or 1.6 eV, which shows that Mn^{3+} in LaMnO_3 is in the HS state, consistent with the reported result [8]. The spectrum of LiMnO_2 in Fig. 2 (a) is in good agreement with the CI theory of $10Dq = 1.7$ eV. This result demonstrates that the Mn^{3+} in LiMnO_2 is a mixture of the HS and LS states, consistent with the result from a similar analysis by de Groot [9]. If the $10Dq$ value of LiMnO_2 is slightly increased by chemical substitution, substrate strain etc., then the Mn^{3+} LS state can be realized in LiMnO_2 , as predicted by first-principle calculations [3].

We also determined the valence of Ni and Cr by XAS spectra. Figure 3 shows the Ni $2p$ XAS spectrum of $\text{LiMn}_{0.5}\text{Ni}_{0.5}\text{O}_2$ and its comparison with the reference data of Ni^{2+} (NiO) and Ni^{3+} (NdNiO_3 and PrNiO_3) from Ref. [10]. The spectrum of $\text{LiMn}_{0.5}\text{Ni}_{0.5}\text{O}_2$ is similar

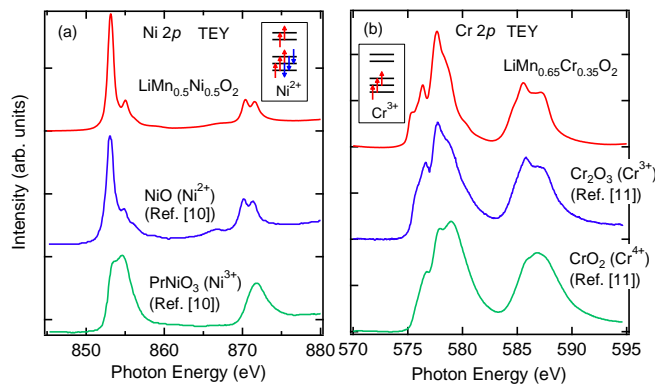


FIG. 3: (Color online) (a) Ni $2p$ XAS spectrum of $\text{LiMn}_{0.5}\text{Ni}_{0.5}\text{O}_2$ and its comparison with the reference data of Ni^{2+} (NiO) and Ni^{3+} (NdNiO_3 and PrNiO_3) from Ref. [10]. The inset shows the electron configuration of Ni^{2+} . (b) Cr $2p$ XAS spectrum of $\text{LiMn}_{0.65}\text{Cr}_{0.35}\text{O}_2$ and its comparison with the reference data of Cr^{3+} (Cr_2O_3) and Cr^{4+} (CrO_2) from Ref. [11]. The inset shows the electron configuration of Cr^{3+} .

to that of NiO rather than NdNiO_3 and PrNiO_3 , indicating that the valence of Ni is $2+$ in $\text{LiMn}_{0.5}\text{Ni}_{0.5}\text{O}_2$. Similarly, it is shown from the Cr $2p$ XAS spectrum of $\text{LiMn}_{0.65}\text{Cr}_{0.35}\text{O}_2$ Fig. ?? and its comparison with the reference data of Cr^{3+} (Cr_2O_3) and Cr^{4+} (CrO_2) from Ref. [11] that our result is similar to that of Cr_2O_3 and the valence of Cr is $3+$ in $\text{LiMn}_{0.65}\text{Cr}_{0.35}\text{O}_2$.

From the above results, we determined that the electronic configurations in powder samples are $\text{LiMn}^{3+}\text{O}_2$, $\text{LiMn}_{0.5}^{4+}\text{Ni}_{0.5}^{2+}\text{O}_2$, and $\text{Li}_x\text{Mn}_{0.65}^{4+}\text{Cr}_{0.35}^{3+}\text{O}_2$. In the Cr-substituted sample, we have to take into account the Li deficiencies to keep the material charge-neutral, and the value of Li concentration x is calculated to be 0.35. Such a large Li deficiency is also concluded from the results of photoemission spectroscopy [12].

When we substitute Cr for Mn in LiMnO_2 , the Cr^{3+} valence and the change from Mn^{3+} to Mn^{4+} introduce Li deficiencies and make this material unsuitable for battery cathodes. In the case of Ni substitution, the Ni^{2+} valence and the change from Mn^{3+} to Mn^{4+} do not create Li deficiencies and the material is suitable for cathodes. When we classify transition-metal compounds in the scheme of Zaanen, Sawatzky and Allen [13, 14], that is as a function of Coulomb repulsion U and charge-transfer energy from O $2p$ states to transition-metal $2p$ states Δ , charge-transfer-type ($\Delta < U$) such as Ni and Cu is more suitable for LiMnO_2 battery cathodes than Mott-Hubbard type ($U < \Delta$) such as Cr because Ni and Cu becomes $2+$ and does not cause Li-deficiencies in the material.

We performed an x-ray absorption study of LiMnO_2 and its related materials and determined the oxidation states of transition-metal ions. The XAS result of LiMnO_2 shows that the Mn^{3+} in LiMnO_2 is a mixture of the HS and LS states, suggesting that small perturba-

tion such as Cr doping in powder samples or substrate strain of thin films may stabilize the LS Mn^{3+} state in LiMnO_2 . In $\text{Li}_x\text{Mn}_{0.65}\text{Cr}_{0.35}\text{O}_2$, although the substituted Cr becomes $3+$ as expected, the Cr doping unfortunately causes Li deficiencies and introduces Mn^{4+} . In contrast, $\text{LiMn}_{0.5}\text{Ni}_{0.5}\text{O}_2$ has substituted Ni of $2+$ and does not include Li deficiencies. Thus we conclude that the substitution of charge-transfer-type Ni or Cu is effective for LiMnO_2 battery materials.

This research was made possible with financial support from the Canadian funding organizations NSERC, CFI, and CIFAR.

* Electronic address: wadati@phas.ubc.ca;
URL: <http://www.geocities.jp/qxbqd097/index2.htm>

- [1] K. Mizushima, P. C. Jones, P. J. Wiseman, and J. B. Goodenough, *Mater. Res. Bull.* **15**, 783 (1980).
- [2] K. Kang, Y. S. Meng, J. Breger, C. P. Grey, and G. Ceder, *Science* **311**, 977 (2006).
- [3] Z.-F. Huang, F. Du, C.-Z. Wang, D.-P. Wang, and G. Chen, *Phys. Rev. B* **75**, 054411 (2007).
- [4] F. Du, Z.-F. Huang, C.-Z. Wang, X. Meng, G. Chen, Y. Chen, and S.-H. Feng, *J. Appl. Phys.* **102**, 113906 (2007).
- [5] A. N. Vasiliev, O. S. Volkova, L. S. Lobanovskii, I. O. Troyanchuk, Z. Hu, L. H. Tjeng, D. I. Khomskii, H.-J. Lin, C. T. Chen, N. Tristan, F. Kretzschmar, R. Klingeler, and B. Buchner, *Phys. Rev. B* **77**, 104442 (2008).
- [6] A. Tanaka, *J. Phys. Soc. Jpn.* **63**, 2788 (1994).
- [7] Based on the crystal structure of these materials, the Mn ion is in a trigonal symmetry, but since the trigonal distortion is small, we consider it a reasonable approximation to calculate using an octahedral symmetry. The parameters in the calculation are the charge-transfer energy from the O $2p$ orbitals to the empty Mn $3d$ orbitals $\Delta = 4.5$ eV, the $3d - 3d$ on-site Coulomb interaction energy denoted $U = 4.0$ eV, and the hybridization strength between the Mn $3d$ and O $2p$ orbitals $V(e_g) = 3.0$ eV.
- [8] M. Abbate, F. M. F. de Groot, J. C. Fuggle, A. Fujimori, O. Strebel, F. Lopez, M. Domke, G. Kaindl, G. A. Sawatzky, M. Takano, Y. Takeda, H. Eisaki, and S. Uchida, *Phys. Rev. B* **46**, 4511 (1992).
- [9] F. M. F. de Groot, *J. Electron Spectrosc. Relat. Phenom.* **61**, 529 (1994).
- [10] M. Medarde, A. Fontaine, J. L. Garcia-Munoz, J. Rodriguez-Carvajal, M. de Santis, M. Sacchi, G. Rossi, and P. Lacorre, *Phys. Rev. B* **46**, 14975 (1992).
- [11] Y. S. Dedkov, A. S. Vinogradov, M. Fonin, C. Konig, D. V. Vyalikh, A. B. Preobrajenski, S. A. Krasnikov, E. Y. Kleimenov, M. A. Nesterov, U. Rudiger, S. L. Molodtsov, and G. Guntherodt, *Phys. Rev. B* **72**, 060401 (2005).
- [12] N. Takaiwa *et al.*, private communication.
- [13] J. Zaanen, G. A. Sawatzky, and J. W. Allen, *Phys. Rev. Lett.* **55**, 418 (1985).
- [14] A. E. Bocquet, T. Mizokawa, K. Morikawa, A. Fujimori, S. R. Barman, K. Maiti, D. D. Sarma, Y. Tokura, and M. Onoda, *Phys. Rev. B* **53**, 1161 (1996).